THE ROYAL SOCIETY

J. R. Soc. Interface (2004) **1**, 79–90
DOI: 10.1098/rsif.2004.0008

Discrimination between ricin and sulphur mustard toxicity *in vitro* using Raman spectroscopy

Ioan Notingher[1,‡], Chris Green[2], Chris Dyer[2], Elaine Perkins[2], Neil Hopkins[2], Chris Lindsay[2] and Larry L. Hench[1,†]

[1]*Department of Materials, Imperial College London, Exhibition Road, London, SW7 2AZ, UK*
[2]*Biomedical Sciences and Detection Departments of Dstl, Porton Down, Salisbury, Wiltshire, SP4 0JQ, UK*

A Raman spectroscopy cell-based biosensor has been proposed for rapid detection of toxic agents, identification of the type of toxin and prediction of the concentration used. This technology allows the monitoring of the biochemical properties of living cells over long periods of time by measuring the Raman spectra of the cells non-invasively, rapidly and without use of labels (Notingher *et al.* 2004 doi:10.1016/j.bios.2004.04.008). Here we show that this technology can be used to distinguish between changes induced in A549 lung cells by the toxin ricin and the chemical warfare agent sulphur mustard. A multivariate model based on principal component analysis (PCA) and linear discriminant analysis (LDA) was used for the analysis of the Raman spectra of the cells. The leave-one-out cross-validation of the PCA–LDA model showed that the damaged cells can be detected with high sensitivity (98.9%) and high specificity (87.7%). High accuracy in identifying the toxic agent was also found: 88.6% for sulphur mustard and 71.4% for ricin. The prediction errors were observed mostly for the ricin treated cells and the cells exposed to the lower concentration of sulphur mustard, as they induced similar biochemical changes, as indicated by cytotoxicity assays. The concentrations of sulphur mustard used were also identified with high accuracy: 93% for 200 µM and 500 µM, and 100% for 1000 µM. Thus, biological Raman microspectroscopy and PCA–LDA analysis not only distinguishes between viable and damaged cells, but can also discriminate between toxic challenges based on the cellular biochemical and structural changes induced by these agents and the eventual mode of cell death.

Keywords: Raman microspectroscopy; living cells; ricin; sulphur mustard; toxicology; biosensor

1. INTRODUCTION

The increased threat of bio-terrorism during the last few years has led to an increased demand for systems able to detect and identify chemical and biological warfare agents and other toxic chemicals. In response to this demand, much effort has been focused on developing biosensors that have the potential to respond to a diverse range of toxic chemicals and biological toxins at relevant concentrations and in real-time. The use of living cells as the sensor elements in such systems is one approach that has undergone significant developments during the last decade with single cells, layers of confluent cells, networks and arrays of living cells being used for proof of principle studies or being incorporated into prototype devices (see recent reviews by Pancrazio *et al.* (1999) and Ziegler (2000)). The potential advantage of such cell-based systems over other types of biosensors, such as molecular, antibody-biosensors for example, is that they are not engineered to respond specifically to a single toxic agent but are free to react to many biologically active compounds.

Of critical importance for such cell-based biosensors is the use of an appropriate method for interrogation of the cellular sensor. Changes in cell behaviour, cell–cell and cell–substrate contact, metabolism or induction of cell death following exposure of the cells to toxic agents can be measured and used to detect the presence of the toxic agents. For example, variations in the intensity of the intrinsic light emitted by bioluminescent bacteria can be used to detect toxic chemicals such as polycyclic aromatic hydrocarbons and phenols (Lee *et al.* 2003; Kim *et al.* 2003). Fluorescent labels have been developed to monitor cellular functions and various technologies have been implemented for high-throughput screening (Fernandes *et al.* 1998). Neurotoxic chemicals can be detected by monitoring active

†Author for correspondence (l.hench@imperial.ac.uk).
‡Current address: University of Edinburgh, School of Engineering and Electronics, The King's Buildings, Edinburgh EH9 3JL, UK.

Received 15 June 2004
Accepted 24 August 2004
Published online 1 October 2004

neuronal networks using microelectrode arrays (Gross *et al.* 1992, 1995; Potter & DeMarse 2001; Chiappalone *et al.* 2003; Pancrazio *et al.* 2004). Changes in the spontaneous electric activity, such as burst duration and frequency, can be measured when neurons (Chiappalone *et al.* 2003; Pancrazio *et al.* 2004) are exposed to various neuroactive drugs and toxins. The extracellular potential of other electrically active cells, such as osteoblasts, can also be measured and related to the presence of various toxic agents (Yang *et al.* 2003). Research from other groups has reported the use of microelectronic pH sensors to monitor the acidity of culture media in the vicinity of living cells (Lorenzelli *et al.* 2003). Cells exposed to toxins known to inhibit membrane ionic pumps show small decreases in the pH which can be detected using integrated microelectronics (Lorenzelli *et al.* 2003). Changes in the pH caused by exposure of bacteria engineered genetically to express various enzymes have also been used for the detection of organophosphate toxins, such as nerve agents (Rainina *et al.* 1996). Confluent layers of endothelial cells grown on ion-selective membranes were able to detect various concentrations of histamine in the culture medium due to increased permeability caused by cell–cell contact alteration and the formation of gaps (May *et al.* 2004). Impedance measurements of cellular arrays have been used to determine the behaviour of various cell types, such as fibroblasts (Giaever & Keese 1993) and endothelial cells (Tiruppathi *et al.* 1992).

The main disadvantage of the above techniques is their inability to discriminate between diverse toxic agents. However, whilst information regarding general toxicity may be useful for classification of a potential agent, identification and quantification are also desirable. With the possible exception of the neuronal network type systems, it has proved difficult to identify and quantify different toxic agents with many of these approaches because the interrogation of the cellular component results in a readout with limited biological information, and thus results in similar changes in the detected signal for many different toxic agents. Furthermore, many of these techniques require invasive methods of cell sampling, complex cellular modifications or use cell types that are difficult to establish in reliable cell-lines. In a recent paper, we reported for the first time the use of Raman microspectroscopy as a non-invasive, label-free tool to monitor lung-derived cells exposed to a toxic chemical (Notingher *et al.* 2004*a*). Spectral changes related to proteins, DNA and lipids were identified and quantified by measuring the area of Raman peaks corresponding to these biopolymers. The Raman spectrum of a cell therefore represents an information rich 'fingerprint' of the overall biochemical composition of the cell; thus, different toxic agents that initiate different cellular responses and biochemical changes should produce distinct changes in the Raman spectra. Therefore, we hypothesized that this technique might have the potential to discriminate between various toxic agents and their concentrations by following the time-dependent spectral changes induced.

The univariate methods used for the analysis of the Raman spectra, such as calculation of certain peak areas using peak fitting routines, are gross methods since the Raman spectra of living cells consist of complex bands formed by overlapping peaks corresponding to different chemical species. Therefore, various assumptions regarding peak position, width and shape have to be made for the analysis. Multivariate statistical methods, however, such as principal component analysis (PCA) and linear discriminant analysis (LDA), are superior tools for analysing Raman spectra of biological samples, as no such *a priori* assumptions are required. PCA and LDA have been successfully used for the discrimination of various cancerous tissues (Stone *et al.* 2000, 2002; Nijssen *et al.* 2002; Hakka *et al.* 2002; Shafer-Peltier *et al.* 2002*a*; Koljenovic *et al.* 2002; Kendall *et al.* 2003; Crow *et al.* 2003; Smith *et al.* 2003), identification of micro-organisms (Maquelin *et al.* 2000, 2003; Choo-Smith *et al.* 2001) and chemical imaging of tissues (Nijssen *et al.* 2002; Shafer-Peltier *et al.* 2002*a*,*b*; Kneipp *et al.* 2003). Similar methods have also been used to study individual living cells, such as the monitoring of differentiation of embryonic stem cells (Notingher *et al.* 2004*b*) and the discrimination of bone cell phenotypes (Notingher *et al.* 2004*c*). PCA and LDA methods have also been used in conjunction with other types of cell-based biosensors, such as monitoring the collective behaviour of neurons (Takahashi 1996).

In this paper we investigate the capability of Raman microspectroscopy to discriminate between the cellular effects of ricin and sulphur mustard, two toxic agents of bioterrorism and chemical warfare (CW) significance. Ricin, a potent and potentially lethal ribosome inactivating protein isolated from the seeds of the castor bean plant (*Ricinus communis*), was infamously implicated in the assassination, in London, of the Bulgarian exile Georgi Markov in 1978. Sulphur mustard was first used in WW1 and more recently in the 1980–88 Iran Iraq war and is still a CW agent of concern. Sulphur mustard is a potent bifunctional alkylating agent that causes debilitating chemical burns to the skin, eyes and respiratory tract. Raman spectra of type II pneumocyte-like cells (A549 cell line) exposed to ricin or to sulphur mustard at various concentrations were acquired and subsequently analysed using the PCA–LDA methods. The prediction accuracy of this biosensor for the identification of the challenge agent and estimation of the concentration used has been assessed using the leave-one-out, cross-validation method of the PCA–LDA model that we built.

2. MATERIALS AND METHODS

2.1. Cell culture

The human alveolar epithelial cell line A549 was obtained from the European Collection of Animal Cell Cultures (ECACC, Porton Down, UK; ECACC No. 86012804). Cells were grown in foetal calf serum-containing media and were passaged as recommended by ECACC. For Raman spectroscopy measurements, cells were plated onto 12 mm MgF_2 discs in six well tissue culture plates at 200 000 cells/well and allowed to adhere and grow for 48–72 h prior to measurements being taken. For cytotoxicity and viability staining, cells were plated in 96 or 24 well plates respectively, at 20 000

and 80 000 cells/well respectively, and allowed to adhere and grow for 48 h prior to exposure to the toxic agent.

2.2. Toxic challenges

Ricin (from *Ricinus communis var. zanzibariensis* which was isolated and purified to give a single band by polyacrylamide gel electrophoresis at Dstl, Porton Down) was stored at −20 °C in aliquots at 1 mg ml^{-1} in phosphate-buffer saline (PBS). For use, ricin was diluted into a serum-free culture medium and cells were exposed to the indicated concentrations for 24 h.

Sulphur mustard (Dstl, Porton Down) was stored at 4 °C as a hexane solution at 100 mg ml^{-1}. For use, sulphur mustard was diluted first into isopropyl alcohol to give a 100 mM solution and subsequently into Dulbecco's PBS (with Ca^{2+} and Mg^{2+}). Cells were exposed to 0.5–1000 µM sulphur mustard as indicated in Dulbecco's PBS for 1 h at 37 °C. This exposure medium was subsequently replaced with a fresh culture medium and the cells were returned to the incubator for 24 h.

2.3. Cytotoxicity and viability staining

Cell viability was measured using 3,[4,5-dimethylthiazol-2-yl]-2,5-diphenyltetrazolium bromide (MTT). MTT was added to the cells to give a final concentration of 0.3 mg ml^{-1}. After incubation at 37 °C for 2 h the medium was removed and the blue formazan precipitate was dissolved in dimethylsulphoxide. The absorbance at 540 nm was used as a measure of cell viability.

For viability staining, control and treated cultures were incubated with 5 µg ml^{-1} Hoechst 33258 for 30 min at 37 °C followed by 5 µg ml^{-1} fluorescein diacetate (FDA) and 5 µg ml^{-1} propidium iodide for 2–5 min. Prior to observation, cells were washed with a HEPES-buffered balanced salt solution (HBBSS) of the following composition (mM): NaCl, 135; KCl, 5; $CaCl_2$, 2; $MgCl_2$, 1; $NaHCO_3$, 5; HEPES, 5; and D-glucose, 10; pH 7.4 with NaOH. Annexin V staining was carried out using Alexafluor-488-labelled annexin V (Molecular Probes). Cells were first incubated with 5 µg ml^{-1} Hoechst 33258 in culture medium for 30 min at 37 °C. The cells were then washed in HBBSS and then exposed to a staining solution containing Alexafluor-488 labelled annexin V (1:20 dilution of the supplied stock) and 5 µg ml^{-1} propidium iodide in HBBSS. Images were acquired using a digital camera (Sony DSC S75) and Zeiss Axiovert 25 and appropriate fluorescence filters to achieve separation of the fluorescent signals.

2.4. Raman spectroscopic measurements

Cells cultured onto 12 mm MgF_2 substrates were placed in an Attofluor cell chamber (Molecular Probes), with a 25 mm MgF_2 window as the base, and placed under the Raman microspectrometer. Cells were maintained in HBBSS during Raman measurements. Raman spectra were collected using a Renishaw RM equipped with a 63 × 0.9 NA water immersion objective (Leica) and a high-power, line-focused NIR laser (Renishaw, 785 nm, 300 mW output) for 120 s integration time. MgF_2 substrates were chosen for their low fluorescence background and low Raman scattering in the 600–1800 cm^{-1} region. Previous studies using inductively coupled plasma (ICP) optical emission spectroscopy and MTT viability tests showed that MgF_2 substrates had low solubility in water solutions. The concentrations of Mg^{2+} and F^- ions were found to be far below the toxic levels for primary human osteoblasts (Notingher *et al.* 2004*c*). A 50 µm spectrograph entrance slit and a 12 pixel width image on the CCD were selected. This gave a spatial resolution, measured using 1 µm diameter polystyrene beads, of 4 µm and 11 µm in the lateral directions and 7 µm in the axial direction.

Spectra were obtained centrally over the nucleus of the cells when visible, or over the estimated geometric centre of the blebbing cells. The numbers of cells analysed were: 49 control cells, 21 ricin treated, 15 for 200 and 500 µM sulphur mustard treated and 40 for 1000 µM sulphur mustard treated. For each cell, a corresponding substrate background spectrum was acquired at the same focal position from an adjacent area of cell-free substrate. Cells were selected for study based on their morphology by brightfield microscopy being characteristic of apoptotic cells (ricin treated and 200 µM sulphur mustard treated). Control cells and cells treated with higher concentrations of sulphur mustard were chosen with the aid of brightfield microscopy as being representative of these populations.

Raman spectra of human serum albumin, DNA RNA and phosphatidylcholine were acquired as described above from 50–80 mg ml^{-1} solutions, or in the case of phosphatidylcholine from undissolved solid immersed in PBS. All compounds were from Sigma-Aldrich (Dorset, UK).

2.5. Data analysis

All data analysis was performed using in-house software written for Matlab® (Mathworks Inc, USA).

2.5.1. Spectra pre-processing. For each cell, the substrate background was subtracted and the fluorescence baseline was eliminated by subtracting a fifth-order polynomial fit through the entire spectrum. The PCA–LDA analysis was performed on the computed second derivative of the background corrected spectra (Savitsky-Golay method, 21 points, second-order polynomial). All second-derivative spectra were normalized using the standard normal variate method (SNV) in which, for each spectrum, the mean was set to zero and the standard deviation was set to one.

2.5.2. Principal component analysis. PCA analysis finds combinations of variables that describe the major trends in the data (Wold *et al.* 1987). This technique reduces the dimensionality of the measurement matrix with the goal to represent the data using a smaller number of factors or principal components (PCs). The scores of corresponding to each PC were calculated as the projections of the entire Raman spectra on the directions defined by the PC loadings. The PCs

that described the most significant variance between the spectra were retained for the analysis and the PCA scores were used as input for the LDA model, while the less significant PCs, describing mostly random noise, were discarded.

2.5.3. Linear discriminant analysis. LDA computes linear combinations of variables to determine directions in the spectral space, discriminant functions (LDs), that maximize the variance between groups and minimize the variance within groups according to Fisher's criterion (Hair 1998). For the validation of the LDA model, the leave-one-out cross-validation was used (Stone 1974). In this method, all spectra except one were used to build a LDA model and then to classify the left out spectrum. This method is repeated so that each spectrum is predicted once.

3. RESULTS AND DISCUSSION

3.1. Cytotoxicity

Ricin caused a marked and potent concentration-dependent cytotoxicity in A549 cultures with results from MTT assays indicating a decrease in cell viability by ∼70% following exposure to the highest concentration of ricin for 24 h (figure 1). Ricin-induced cell death was characterized by a gradual contraction of the cell margins and blebbing of the cells. The staining of the ricin-treated cultures with the DNA binding dye Hoechst 33258 revealed extensive condensation of the nuclear chromatin and morphological fragmentation of the cellular nuclei, classical indications of apoptotic cell death (figure 2). Early apoptotic cells retained the ability to accumulate intracellular fluorescein following incubation with FDA and to exclude the DNA binding dye PI indicating an intact plasma membrane. Late apoptotic or necrotic cells did stain with PI and lost their ability to accumulate fluorescein (figure 2).

Sulphur mustard also produced a concentration-dependent cytotoxicity in A549 cells (figure 1). The morphological features of this cytotoxicity depended greatly on the concentration of sulphur mustard used. Immediately after the addition of the 200 µM sulphur mustard, the majority of the cells had a normal morphology. However, following the 24 h incubation in normal culture medium, there was a decrease in the cell viability by approximately 50% and the number of condensed and blebbing cells increased (figures 3 and 4). Many of these cells stained with FDA, contained condensed fragmented nuclear chromatin and excluded PI suggesting an apoptotic cell death. Additionally, these cells also stained positively for externalized phosphatidylserine, a marker of early apoptosis (figure 4). At 500 µM, sulphur mustard induced rounding of the A549 cells, with many cells detaching from the substrate. Following wash-off of the sulphur mustard and 24 h incubation in complete culture medium, these cells still appeared abnormal and rounded (figure 4). However, many of these cells remained viable according to their ability to accumulate FDA and exclude PI (data not shown). Treatment of the A549 cells with the highest concentration of sulphur mustard, 1000 µM, resulted in early morphological changes including rapid lysis of cells and the appearance of large membrane blebs that were evident at the end of the exposure period. This morphology was remarkably stable over the 24 h incubation following the 1 h exposure. Figure 4 shows that the treated cells stained strongly with alexafluor-488-annexin V and with PI, indicating compromised plasma membranes and thus free access of the dyes in internal membranes.

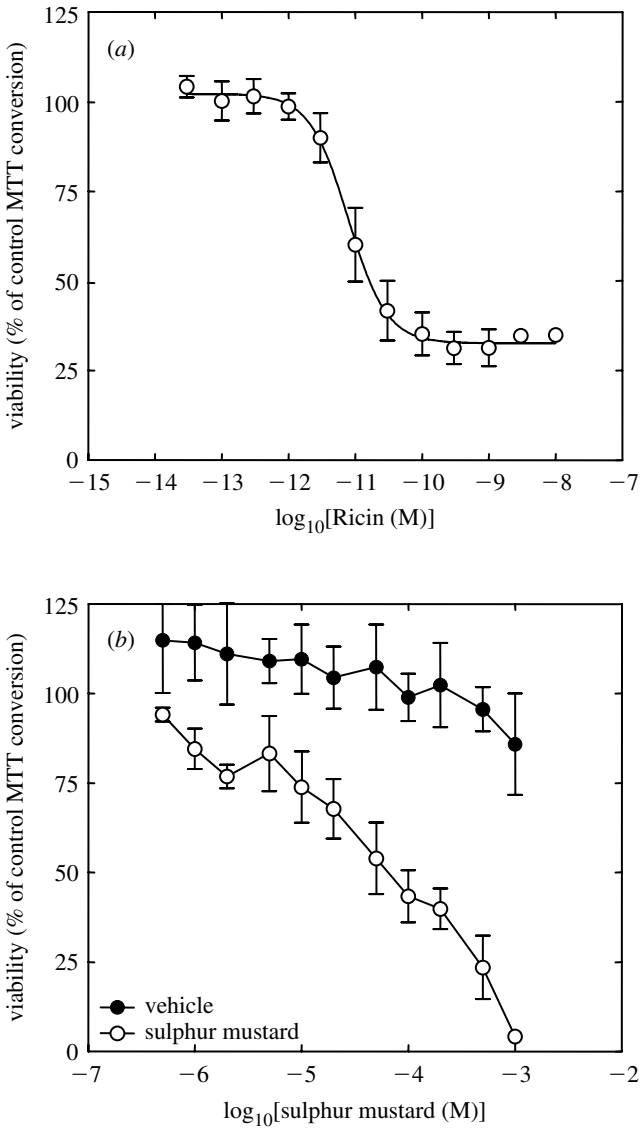

Figure 1. Concentration dependence of ricin (*a*) and sulphur mustard (*b*) induced cytotoxicity. The curve in (*a*) was fitted with a four-parameter logistic equation using GraphPad Prism.

3.2. Raman spectroscopy

The pre-processed averaged Raman spectra of healthy A549 cells and A549 cells treated with ricin and sulphur mustard are presented in figure 5. All Raman spectra showed features similar to the Raman spectra of A549 (Notingher *et al.* 2003; Verrier *et al.* 2004) and other cell types (Puppels *et al.* 1990; Uzunbajakava *et al.* 2003*a*,*b*;

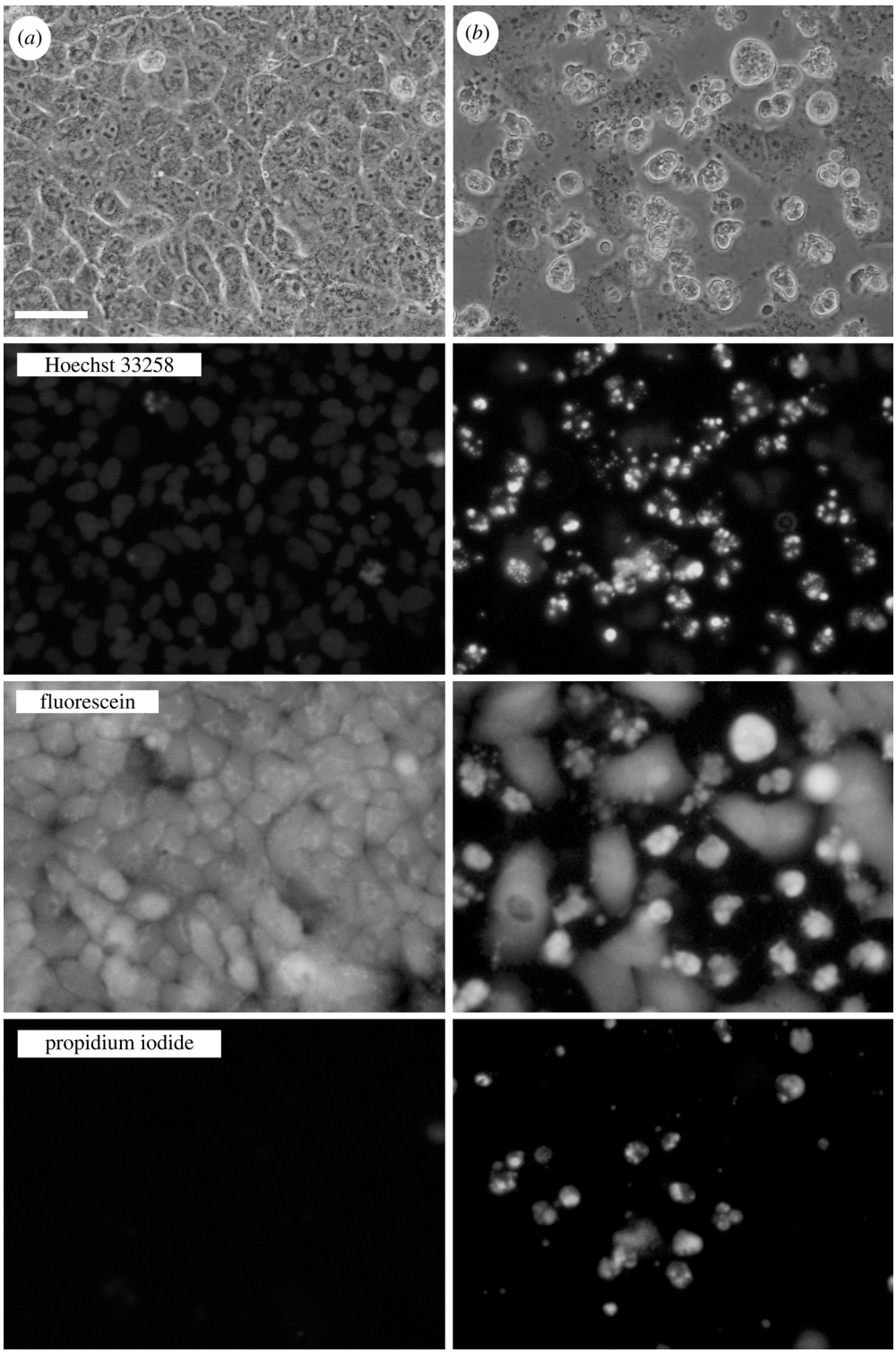

Figure 2. Viability staining of control (*a*) and ricin-treated (*b*) A549 cells. Cells were stained with FDA, PI and Hoechst 33258 as described in the methods. Phase contrast and fluorescence images are all of the same field of view. (Scale bar = 30 µm.)

Krafft *et al.* 2003; Notingher *et al.* 2004*a–c*) reported previously. Contributions corresponding to all major cellular biopolymers, i.e. proteins, DNA, RNA, lipids and carbohydrates, can be identified (Tu 1982; Gremlich and Yan 2001), as summarized in table 1 (see also figure 6). Proteins have strong Raman peaks at 1660 cm^{-1} (Amide I), 1200–1300 cm^{-1} (Amide III), 1005 cm^{-1} (phenylalanine) and 1449 cm^{-1} (C–H vibrations). The main Raman peaks of nucleic acids correspond to the phosphate–sugar backbone vibrations, such as the 1095 cm^{-1} (phosphodioxy group PO_2^-), 788 cm^{-1} (C_5'–O–P–O–C_3' phosphodiester bonds in DNA) and 813 cm^{-1} (C_5'–O–P–O–C_3' phosphodiester bonds in RNA) and to the nuclear bases, such as 782 cm^{-1} (thymine, cytosine and uracil) and 1578 cm^{-1} (guanine and adenine). Lipids have strong Raman peaks at

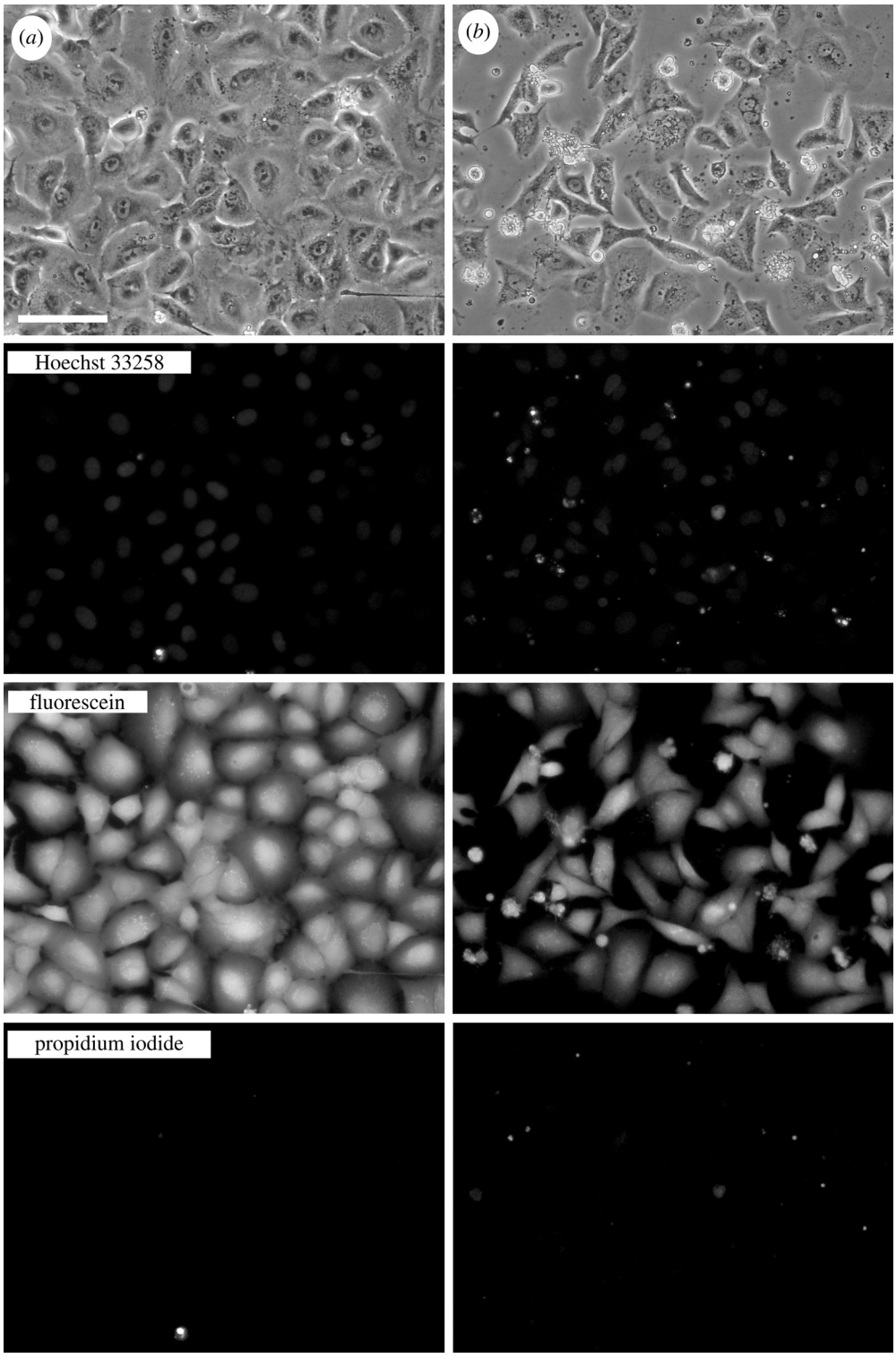

Figure 3. Viability staining of control (*a*) and 200 µM sulphur mustard-treated (*b*) A549 cells. Cells were stained with FDA, PI and Hoechst 33258 as described in the methods. Phase contrast and fluorescence images are all of the same field of view. (Scale bar = 50 µm.)

1449 cm^{-1}, 1301 cm^{-1} (C-H vibrations) and 1660 cm^{-1} (C=C stretching). A strong peak at 719 cm^{-1} can also be observed, which corresponds to the C–C–N^+ symmetric stretching in phosphatidylcholine, one of the major constituents of cellular membranes.

The averaged difference spectra between the Raman spectra of healthy A549 cells and the A549 cells subjected to toxic challenges are shown in figure 6, alongside the Raman spectra of pure DNA, RNA, human serum albumin and phosphatidylcholine. The difference Raman spectra suggest that there are similarities between the spectral changes of A549 cells treated with ricin and the lower concentrations of sulphur mustard (200–500 µM) compared to high concentrations of sulphur mustard (1000 µM). Since the two cell death mechanisms (apoptosis and necrosis) involve

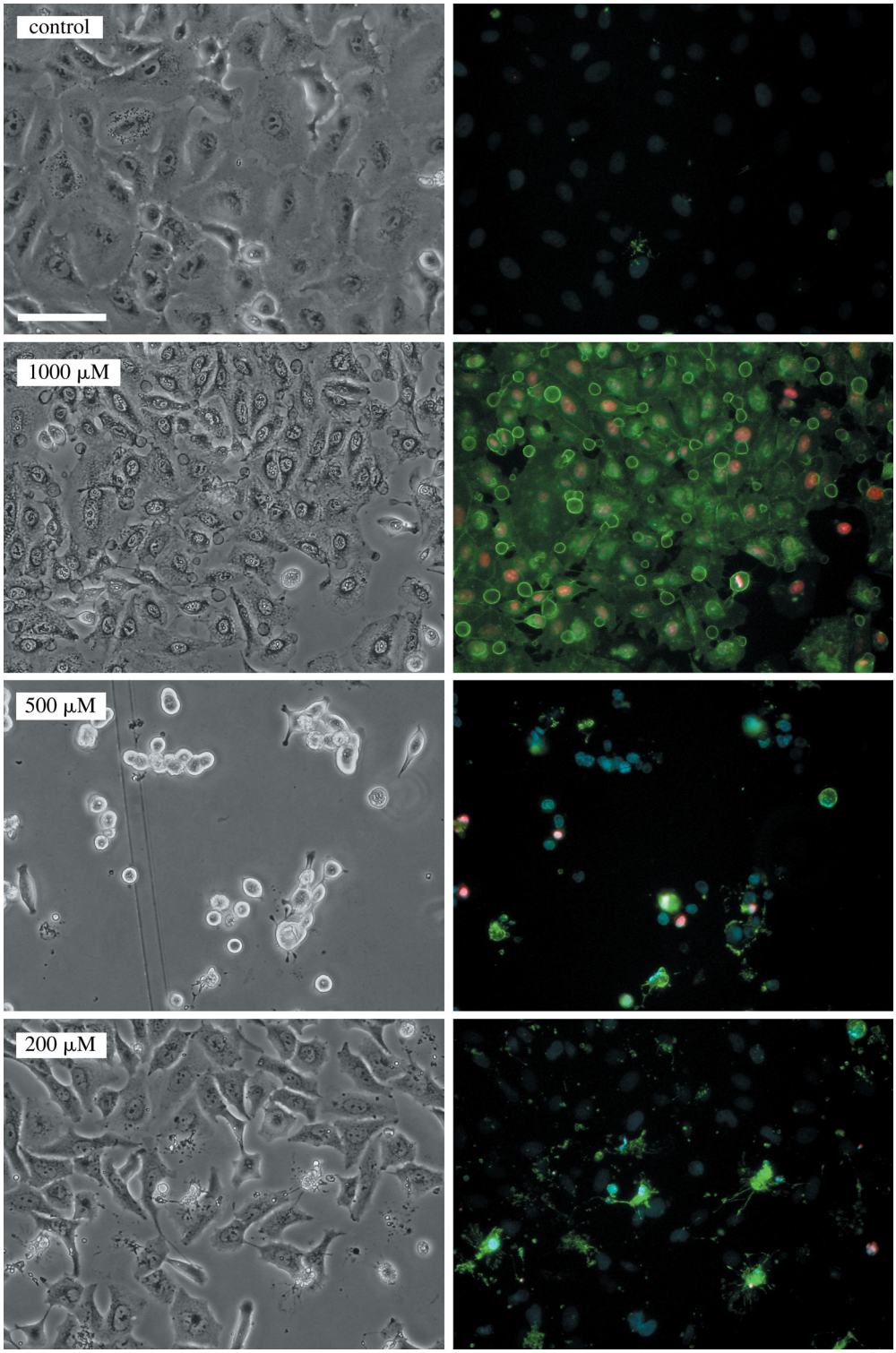

Figure 4. Phase contrast and fluorescence (Annexin V, Hoechst 33258 and propidium iodide) micrographs of A549 cells exposed to sulphur mustard. Cells were exposed to the indicated concentration of sulphur mustard as described in the methods. Micrographs were taken 24 h after exposure. Fluorescence images are composites of three pseudocoloured images of Annexin V (green), Hoechst 33258 (blue) and propidium iodide (red). Images were pseudocoloured and combined using Adobe Photoshop. (Scale bar = 50 μm.)

different biochemical processes, the measured spectral changes can be used as discriminating signatures for the two toxic agents and may also be used to determine the concentration of the toxic agents. The A549 cells undergoing apoptosis showed a relative decrease in the Raman peaks corresponding to DNA (782 cm^{-1} and 788 cm^{-1}, DNA) and proteins (1005 cm^{-1}, HSA), and an increase in the Raman peaks corresponding to lipids (1301 cm^{-1}, 1449 cm^{-1}, 1660 cm^{-1}) (peaks marked by $*$ in figure 6). In comparison, the necrotic A549 cells treated with the highest concentration of sulphur mustard showed no apparent changes in the

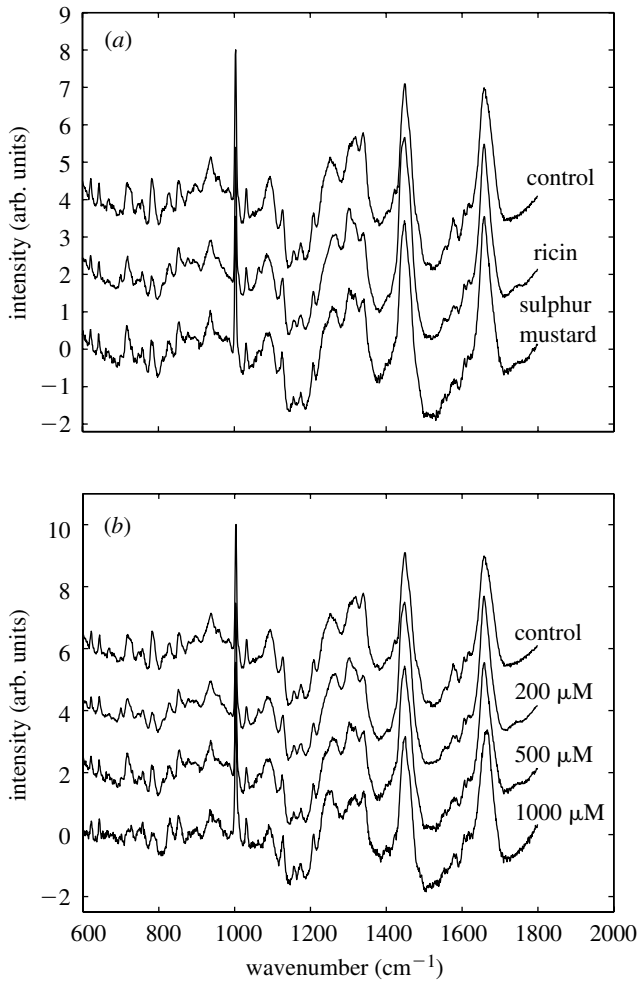

Figure 5. Averaged Raman spectra of A549 cells: (*a*) control, treated with 10 nM ricin and treated with 500 μM sulphur mustard; (*b*) exposed to sulphur mustard at various concentrations. (Spectra have been base-line corrected, SNV normalized and shifted vertically for clarity).

Raman peaks corresponding to DNA and lipids but a decrease in the peaks corresponding to RNA (782 and 813 cm^{-1}, RNA), and an increase in the protein peaks (1005) (peaks marked by + in figure 6).

The spectral changes observed in the Raman spectra of A549 cells subjected to toxic challenges can be correlated to intracellular biochemical changes. In apoptotic cells major changes in the structure, packaging and integrity of nuclear DNA occur as do changes in cytoplasmic biochemistry and cell volume, yet cellular membranes including the plasma membrane can remain intact for prolonged periods (see figure 2). These features of apoptosis could therefore be responsible for the observed relative decrease in the concentrations of DNA and proteins with respect to the lipid concentration. However, the changes related to the peaks of lipids and proteins in the Raman spectra of necrotic cells are more difficult to explain. Necrotic cells would be expected to lose cytoplasmic protein upon plasma membrane lysis; indeed, this effect has been observed using Raman spectroscopy in Triton-X-100-lysed A549 cells (Green, Dyer and Perkins, unpublished observations). The reason why these changes were not observed may be due to the ability of sulphur mustard, a bifunctional alkylating agent, to cross-link proteins thus potentially 'fixing' the cells. It is also important to note here that, as a consequence of the normalization methods used, changes in absolute concentrations of cellular constituents within the sampling volume are lost and the changes reported are relative changes in the cellular composition.

Although the interpretation of the spectral changes observed in figure 6 is not straightforward, these changes might be sufficient to detect, identify and to estimate the concentration of a toxic agent. To test this hypothesis, PCA–LDA analysis was applied to the data. The first step for the discrimination analysis was to determine the most relevant principal components in the PCA analysis of the Raman spectra of all cells, prior to data compression and input for the LDA analysis. Only the first six PCs were retained for the LDA analysis (captured 39.63% of the variance between the mean-centred spectra of all cells), since the loadings of the higher-order PCs had low signal-to-noise ratios.

The following scheme was adopted for determining the capability of the biological Raman spectroscopy and PCA–LDA model to discriminate between ricin and sulphur mustard treated cells, and to discriminate between various sulphur mustard concentrations. The first step was the discrimination of damaged cells from healthy cells, which is achieved by determining the discriminant function LD1; the next step was to discriminate between ricin and sulphur mustard (LD2) using all cells known to be damaged. Lastly, the cells challenged by sulphur mustard were further analysed to predict the concentration used (LD3 and LD4). The results of the leave-one-out, cross-validation method used in conjunction with this scheme are shown in table 2 and graphical representations of the relationships between the linear discriminant functions are shown in figure 7.

Figure 7*a* presents the PCA–LDA scores corresponding to LD1 and LD2 of all the A549 cells analysed. The formation of three analytical clusters is observed, corresponding to healthy A549 cells, ricin-treated A549 cells and sulphur-mustard-treated A549 cells. While the cluster of the healthy A549 cells is well separated (except for five cells), some overlapping between the cells treated with ricin and low concentrations of sulphur mustard can be observed. The PCA–LDA scores corresponding to LD3 and LD4 for the discrimination between the effects of different concentrations of sulphur mustard on the A549 cells are presented in figure 7*b*. The analytical clusters corresponding to all treatment groups are well separated, except two cells treated with 200 μM sulphur mustard being close to the cluster corresponding to the A549 cells treated with 1000 μM sulphur mustard.

The high discrimination power of the Raman spectroscopy combined with the PCA–LDA method suggested by the distinctive analytical clusters observed in the LD1 versus LD2 and LD3 versus LD4 plots (figure 7*a* and *b*) can be tested using the well-established method of leave-one-out cross-validation (Stone 1974). The results of the cross-validation analysis are summarized in table 2. The first discriminating function

Table 1. Peak assignment of the Raman spectra of A549 cells.

	Assignment			
Peak (cm^{-1})	DNA/RNA	Proteins	Lipids	Carbohydrates
1736			C=O ester	
1680–1655		Amide I	C=C str.	
1617		C=C Tyr, Trp		
1607		C=C Phe, Tyr		
1578	G, A			
1480–1420	G, A, CH def	CH def	CH def	CH def
1342	A, G	CH def		CH def
1320	G	CH def		
1301			CH_2 twist	
1284–1220	T, A	Amide III	=CH bend	
1209		$C–C_6H_5$ str. Phe, Trp		
1176		C–H bend Tyr		
1158		C–C/C–N str.		
1128		C–N str.		C–O str.
1095–1060	PO_2^- str.		Chain C–C str.	C–O, C–C str.
1033		C–H in-plane Phe		
1005		Sym. ring br. Phe		
980		C–C BK str. β-sheet	=CH bend	
937		C–C BK str. α-helix		C–O–C glycos.
877			$C–C–N^+$ sym. str.	C-O-C ring
854		Ring br. Tyr		
828	O–P–O asym.str.	Ring br. Tyr		
811	O–P–O str. RNA			
788	O–P–O str. DNA			
782	U,C,T ring br.			
760		Ring br. Trp		
729	A			
717			$CN^+(CH_3)_3$ str.	
667	T, G			
645		C–C twist Tyr		
621		C–C twist Phe		

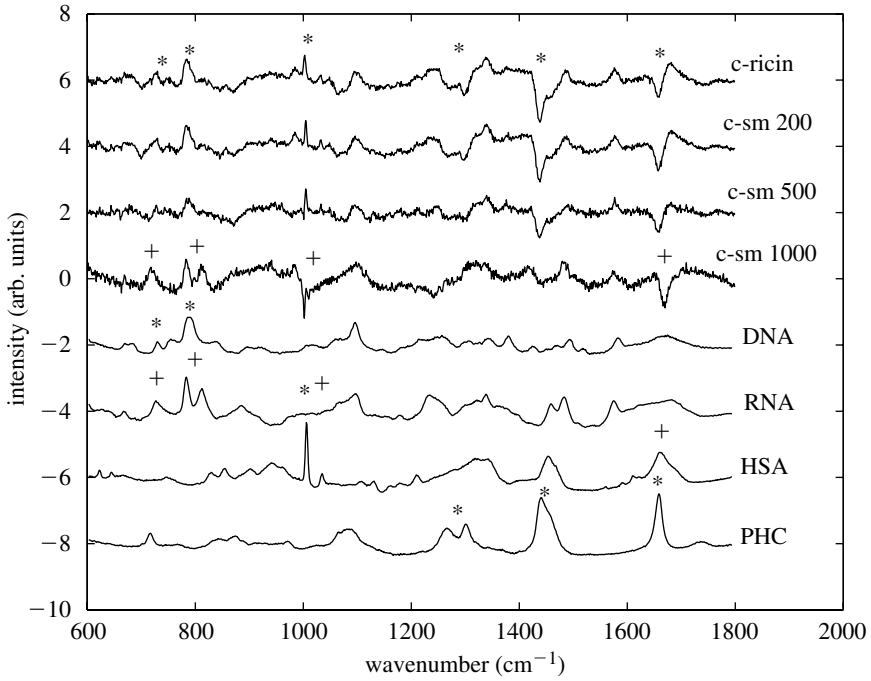

Figure 6. Differences between Raman spectra of control A549 cells and A549 cells treated with 10 nM ricin, 200 µM, 500 µM or 1000 µM sulphur mustard compared to the reference Raman spectra of DNA, RNA, human serum albumin (HAS) and phosphatidylcholine (PHC). ∗ spectral changes associated to apoptosis; +, spectral changes associated to necrosis. (Spectra are shifted vertically for clarity; c, control; sm, sulphur mustard.)

Table 2. Classification accuracy of the PCA–LDA model by the leave-one-out, cross-validation method (note that the sulphur-mustard-treated cells predicted as ricin-treated cells (total of eight): six were 200 µM, two were 500 µM).

	Classification								
True class	Healthy	Damaged	Ricin	Sulphur mustard	Sulphur mustard 200 µM	Sulphur mustard 500 µM	Sulphur mustard 1000 µM	Total cell number	Correct class (%)
Healthy	43	6						49	87.7
Damaged	1	90						91	98.9
Ricin			15	6				21	71.4
Sulphur mustard			8	62				70	88.6
Sulphur mustard 200 µM					14	1	0	15	93.3
Sulphur mustard 500 µM					1	14	0	15	93.3
Sulphur mustard 1000 µM					0	0	40	40	100

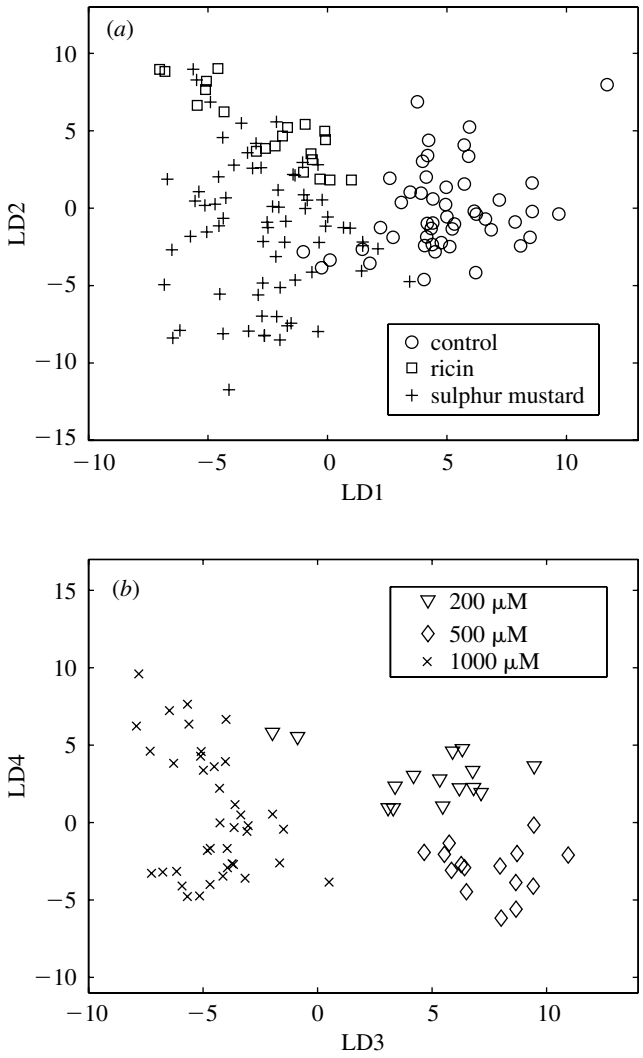

Figure 7. PCA-LDA scores of: (*a*) control A549 cells and all A549 cells treated with ricin (10 nM) and sulphur mustard for 24 h; (*b*) A549 cells treated with various 200 µM, 500 µM and 1000 µM sulphur mustard.

LD1 showed that the damaged cells can be detected with 98.9% sensitivity (90 out of 91 damaged cells) and 87.7% specificity (43 out of 49 healthy cells). The second test for identification of the toxic agent used (LD2) showed that 88.6% of the cells treated with sulphur mustard and 71.4% of the cells treated with ricin were correctly classified. From the total of eight A549 cells incorrectly predicted as being exposed to ricin, six were treated with 200 µM and two with 500 µM. These errors in the prediction of the toxic agent used are most probably due to the fact that ricin and sulphur mustard at low concentrations induced similar apoptotic changes in the A549 cells (see figure 4) and similar changes in Raman spectra (figure 6). However, we have only examined a single time point in these studies and the possibility of examining time-dependent changes with Raman spectroscopy (Notingher *et al.* 2004*a*) could lead to better discrimination between agents which have similar apoptotic or necrotic endpoints. Discriminant functions LD3 and LD4 showed that the concentrations of sulphur mustard could be predicted with high accuracy; the percentage of cells classified correctly was 93.3% for the 200 µM and 500 µM and 100% for the 1000 µM concentrations. The high prediction accuracy (100% sensitivity) achieved for the A549 cells exposed to the highest concentration of sulphur mustard is because sulphur mustard at 1000 µM induced very different spectral changes (figure 6) due to the induction of necrotic type cell death rather than apoptosis (figures 3 and 4).

4. CONCLUSIONS

This study shows that application of Raman microspectroscopy to the study of living cells is an effective non-invasive, label-free, sampling method which, when combined with multivariate statistical methods of spectral analysis, is able to detect the damage induced in A549 cells by two highly toxic agents, ricin and sulphur mustard. The leave-one-out cross-validation of the PCA–LDA analysis showed that damaged cells can be detected with high sensitivity (98.9%) and high specificity (87.7%). Moreover, this method showed high accuracy in identifying the nature of the toxic agent, as 88.6% of the cells treated with sulphur mustard and 71.4% of the cells exposed to ricin were classified correctly. The similarity between the spectroscopic changes caused by cellular modifications induced by ricin and sulphur mustard at low concentrations (200 µM) were responsible for most of the prediction errors. The potential of the Raman microspectroscopy to discriminate between concentration-dependent effects of sulphur

mustard on A549 cells was also demonstrated, as different cell-death mechanisms were observed: 200 µM and 500 µM sulphur mustard induced apoptosis, while at 1000 µM necrosis was observed. The two cell-death mechanisms also induced distinct changes in the Raman spectra of A549 cells, as indicated by the computed difference spectra. The A549 cells exposed to sulphur mustard in the 200–1000 µM range were correctly identified with a precision higher that 90% (93% for 200 µM and 500 µM, and 100% for 1000 µM).

The main advantage of this technology is that it allows the monitoring of the biochemical properties of the same cells over long periods of time since no labels, cellular modifications or invasive methods are required to obtain the Raman spectra of the cells (Notinger *et al.* 2004a). This technology could also be applied to other cellular studies, such as interactions between cells and drugs, toxic chemicals, substrate materials or early detection of cancerous/abnormal cells in explants or *in vitro* studies. Future work will establish spectral signatures of other toxic agents, such as organophosphate pesticides, nerve agents and other toxins of bioterrorism and CW relevance, to further characterize the discriminant power of this approach and to provide data that could be used subsequently for the detection, identification and quantification of a large range of toxic agents. Moreover, time course experiments will be carried out because spectroscopic monitoring of cells during the early stages of exposure to toxic agents may increase the discrimination power of this technique. Early time-dependent cellular responses are more likely to depend on the type and concentration of the toxic agent than the final cell death mechanism, apoptosis or necrosis.

The authors wish to acknowledge the financial support of the US Defence Advanced Research Projects Agency (contract No. N66001-C-8041).

REFERENCES

Chiappalone, M., Vato, A., Tedesco, M. B., Marcoli, M., Davide, F. & Martinoia, S. 2003 Networks of neurons coupled to microelectrode arrays: a neuronal sensory system for pharmacological applications. *Biosens. Bioelectron.* **18**, 627–634.

Choo-Smith, L.-P. *et al.* 2001 Investigating microbial (micro)colony heterogeneity by vibrational spectroscopy. *Appl. Environ. Microbiol.* **67**, 1461–1469.

Crow, P., Stone, N., Kendall, C. A., Uff, J. S., Farmer, J. A., Barr, H. & Wright, M. P. 2003 The use of Raman spectroscopy to identify and grade prostatic adenocarcinoma in vitro. *Br. J. Cancer.* **89**, 106–108.

Fernandes, P. B. 1998 Technological advances in high-throughput screening. *Curr. Opin. Chem. Biol.* **2**, 597–603.

Giaever, I. & Keese, C. R. 1993 A morphological biosensor for mammalian cells. *Nature* **366**, 591–592.

Gremlich, H. U. & Yan, B. 2001 *Infrared and Raman spectroscopy of biological materials.* New York: Marcel Dekker.

Gross, G. W., Rhoades, B. K. & Jordan, R. J. 1992 Neural networks for biochemical sensing. *Sens. Actuators* **6**, 1–8.

Gross, G. W., Azzazy, H. M. E., Wu, M. C. & Rhodes, B. K. 1995 The use of neuronal networks on microelectrode arrays as biosensors. *Biosens. Bioelectron.* **10**, 553–567.

Hair, J. F. 1998 *Multivariate data analysis.* Upper Saddle River: Pearson US Imports & PHIPEs.

Haka, A. S., Shafer-Peltier, K. E., Fitzmaurice, M., Crowe, J., Dasari, R. R. & Feld, M. S. 2002 Identifying microcalcifications in benign and malignant breast lesions by probing differences in their chemical composition using Raman spectroscopy. *Cancer Res.* **62**, 5375–5380.

Lee, H. J., Villaume, J., Cullen, D. C., Kim, B. C. & Gu, M. B. 2003 Monitoring and classification of PAH tocixity using an immobilised bioluminescent bacteria. *Biosensens. Bioelectron.* **18**, 571–577.

Lorenzelli, L., Margesin, B., Martinoia, S., Tedesco M. T. & Valle, M. 2003 Bioelectrochemical signal monitoring og in-vitro cultured cells by means of an automated microsystem based on solid state sensor. *Biosens. Bioelectron.* **18**, 621–627.

Kendall, C., Stone, N., Shepherd, N., Geboes, K., Warren, B., Bennett, R. & Barr, H. 2003 Raman spectroscopy, a potential tool for the objective identification and classification of neoplasia in Barrett's oesophagus. *J. Pathol.* **200**, 602–609.

Kim, B. C., Park, K. S., Kim, S. D. & Gu, M. B. 2003 Evaluation of a high throughput toxicity biosensor and comparison with Daphnia magna bioassay. *Biosens. Bioelectron.* **18**, 821–826.

Koljenovic, S., Choo Smith, L.-P., Bakker Schut, T. C., Kros, J. M., Van der Berge, J. & Puppels, G. J. 2002 Discriminating vital tumor from necrotic tissue in human glioblastoma tissue samples by Raman spectroscopy. *Lab. Invest.* **82**, 1265–1277.

Kneipp, J., Bakker Schut, T., Kliffen, M., Menke-Pluijmers, M. & Puppels, G. 2003 Characterisation of breast duct epithelia: a Raman spectroscopic study. *Vib. Spectrosc.* **32**, 67–74.

Krafft, C., Knetschke, T., Siegner, A., Funk, R. H. W. & Salzer, R. 2003 Mapping of single cells by near infrared Raman microspectroscopy. *Vib. Spectrosc.* **32**, 75–83.

Maquelin, K., Choo-Smith, L.-P., van Vreeswijk, T., Endtz, H. P., Smith, B., Bennett, R., Bruining, H. A. & Puppels, G. J. 2000 Raman spectroscopic method for identification of clinically relevant microorganisms growing on solid culture medium. *Anal. Chem.* **72**, 12–19.

Maquelin, K., Kirschner, C., Choo-Smith, L.-P., Ngo-Thi, N. A., van Vreeswijk, T., Stämmler, M., Endtz, H. P., Bruining, H. A., Naumann, D. & Puppels, G. J. 2003 Prospective study of the performance of vibrational spectroscopies for rapid identification of bacterial and fungal pathogens recovered from blood cultures. *J. Clin. Microbiol.* **41**, 324–329.

May, K. M. L., Wang, Y., Bachas, L. G. & Anderson, K. W. 2004 Development of a whole-cell-based biosensor for detecting histamine as a model toxin. *Anal. Chem.* **76**(14), 4156–4161. (doi:10.1021/ac049810+).

Nijssen, A., Bakker Schut, T. C., Heule, F., Caspers, P. J., Hayes, D. P., Neumann, M. H. A. & Puppels, G. J. 2002 Discriminating basal cell carcinoma from its surrounding tissue by Raman spectroscopy. *J. Invest. Dermatol.* **119**, 64–64.

Notingher, I., Verrier, S., Haque, S., Polak, J. M. & Hench, L. L. 2003 Spectroscopic study of human lung epithelial cells (A549) in culture: living cells versus dead cells. *Biopolymers* **72**, 230–240.

Notingher, I., Selvakumaran, J. & Hench, L. L. 2004*a* New detection system for toxic agents based on continuous spectroscopic monitoring of living cells. *Biosens. Bioelectron.* (In the press). (doi:10.1016/j.bios.2004.04.008).

Notingher, I., Bisson, I., Bishop, A. E., Randle, W. L., Polak, J. M. P. & Hench, L. L. 2004*b* In-situ monitoring of mRNA translation in embryonic stem cells during differentiation in-vitro. *Anal. Chem.* **76**, 3185–3193.

Notingher, I., Jell, G., Lohbauer, U., Salih, V. & Hench, L. L. 2004*c* In-situ non-invasive spectral discrimination between bone cell phenotypes used in tissue engineering. *J. Cell. Biochem.* **92**, 1180–1192.

Pancrazio, J. J., Whelan, J. P., Borkholder, D. A., Ma, W. & Stenger, D. A. 1999 Development and applications of cell-base biosensors. *Ann. Biomed. Eng.* **27**, 697–711.

Pancrazio, J. J., Kulagina, N. V., Shaffer, K. M., Gray, S. A. & O'Shaughnessy, T. J. 2004 Sensitivity of the neuronal network biosensor to environmental threats. *J. Toxicol. Env. Heal.* A **67**, 809–818.

Potter, S. & DeMarse, T. B. 2001 A new approach to neural cell culture for long-term studies. *J. Neurosci. Methods* **110**, 17–24.

Puppels, G. J., de Mul, F. F., Otto, C., Greve, J., Robert-Nicoud, M., Arndt-Jovin, D. J. & Jovin, T. M. 1990 Studying single living cells and chromosomes by confocal Raman microspectroscopy. *Nature* **347**, 301–303.

Rainina, E. I., Efremenco, E. N., Varfolomeyev, S. D., Simonian, A. L. & Wild, J. R. 1996 The development of a new biosensor based on recombinant E. coli for the direct detection of organophosphorus neurotoxins. *Biosens. Bioelectron.* **11**, 991–1000.

Shafer-Peltier, K. E., Haka, A. S., Fitzmaurice, M., Crowe, J., Myles, J., Dasari, R. R. & Feld, M. S. 2002*a* Raman microscopic model of human breast tissue: implications for breast cancer diagnosis in vivo. *J. Raman. Spectrosc.* **33**, 552–563.

Shafer-Peltier, K. E., Haka, A. S., Motz, J. T., Fitzmaurice, M., Dasari, R. R. & Feld, M. S. 2002*b* Model-based biological Raman spectral imaging. *J. Cell. Biochem.* **39**, 125–137.

Smith, J., Kendall, C., Sammon, A., Christie-Brown, J. & Stone, N. 2003 Raman spectral mapping in the assessment of axillary lymph nodes in breast cancer. *Technol. Cancer. Res. Treat.* **2**, 327–332.

Stone, M. 1974 Cross-validatory choice and assessment of statistical assessment of statistical predictions. *J. Royal. Stat. Soc.* B **36**, 111–147.

Stone, N., Stavroulaki, P., Kendall, C., Birchall, M. & Barr, H. 2000 Raman spectroscopy for early detection of laryngeal malignancy: preliminary results. *Laryngoscope* **110**, 1756–1763.

Stone, N., Kendall, C., Shepherd, N., Crow, P. & Barr, H. 2002 Near-infrared Raman spectroscopy for the classification of epithelial pre-cancers and cancers. *J. Raman Spectrosc.* **33**, 564–573.

Takahashi, T. 1996 Two statistical methods for analysing multiple neuronal data. *Int. J. Neurosci.* **88**, 11–26.

Tiruppathi, C., Malik, A. B., Del Vecchio, P. J., Keese, C. R. & Giaever, I. 1992 Electrical method for detection of endothelial cell shape change in real time: assessment of endothelial barrier function. *Proc. Natl Acad. Sci. USA* **89**, 7919–7023.

Tu, A. T. 1982 *Raman spectroscopy in biology: principles and applications*. New York: John Wiley and Sons.

Uzunbajakava, N., Lenferink, A., Kraan, Y., Willekens, B., Vrensen, G., Greve, J. & Otto, C. 2003*a* Nonresonant Raman imaging of protein distribution in single human cells. *Biopolymers* **72**, 1–9.

Uzunbajakava, N., Lenferink, A., Kraan, Y., Volokhina, E., Vrensen, G., Greve, J. & Otto, C. 2003*b* Non-resonant confocal Raman imaging of DNA and protein distribution in apoptotic cells. *Biophys. J.* **84**, 3968–3981.

Verrier, S., Notingher, I., Polak, J. M. & Hench, L. L. 2004 In-situ monitoring of cell death using Raman microspectroscopy. *Biopolymers* **74**, 157–162.

Wold, S., Esbensen, K. & Geladi, P. 1987 Principal components analysis. *Chemo. Intell. Lab. Syst.* **2**, 37–52.

Yang, M., Prasad, S., Zhang, X., Morgan, A., Ozkan, M. & Ozkan, C. S. 2003 Cellular microarrays for chemical sensing. *Sensor Mater.* **15**, 313–333.

Ziegler, C. 2000 Cell-based biosensors. *Fresenius J. Anal. Chem.* **366**, 552–559.